J Mater Sci: Mater Electron (2013) 24:4346–4350
DOI 10.1007/s10854-013-1409-6

$(K_{0.5}Na_{0.5})NbO_3$–$Bi(Mg_{0.5}Ti_{0.5})O_3$ solid solution: phase evolution, microstructure and electrical properties

Fen He · Xiuli Chen · Jie Chen · Yiliang Wang · Huanfu Zhou · Liang Fang

Received: 10 May 2013 / Accepted: 23 July 2013 / Published online: 3 August 2013

Abstract Lead-free piezoelectric ceramics with the composition of $(1 - x)(K_{0.5}Na_{0.5})NbO_3$–$xBi(Mg_{0.5}Ti_{0.5})O_3$ [$(1 - x)$KNN–xBMT, $0 \leq x \leq 0.04$] were synthesized via solid-state reaction method. X-ray diffraction patterns revealed that the orthorhombic—tetragonal phase transition was present for $(1 - x)$KNN–xBMT with increasing the content of BMT. The study of dielectric properties illustrated that both peaks of orthorhombic—tetragonal (T_{O-T}) and tetragonal—cubic (T_{T-C}) phase transitions shifted to lower temperature. Through adding BMT, the electrical properties of KNN ceramics were obviously improved. The optimized piezoelectric and ferroelectric properties with $d_{33} = 127$ pC/N, $k_p = 36.58$ %, $P_r = 22.1$ μC/cm^2 were obtained as $x = 0.01$.

1 Introduction

With increasing the environmental protection consciousness, lead-free piezoelectric ceramics with good electrical properties have attracted considerable attention. Among the great number of lead-free piezoelectric ceramics, $(K_{0.5}Na_{0.5})NbO_3$ (KNN) is the most promising candidate and most studied system for its potential piezoelectric properties and high Curie temperature ($T_C \sim 420$ °C) [1–4]. However, it is very difficult to obtain a dense KNN ceramic using conventional sintering process, because of the large volatility of alkaline elements at high temperatures.

F. He · X. Chen (✉) · J. Chen · Y. Wang · H. Zhou · L. Fang
Guangxi Scientific Experiment Center of Mining, Metallurgy and Environment, Key Laboratory of New Processing Technology for Nonferrous Metals and Materials, Ministry of Education, College of Materials Science and Engineering, Guilin University of Technology, Guilin 541004, China
e-mail: cxlnwpu@163.com

Many techniques, including hot pressing [5], spark plasma sintering (SPS) [6–9], are used to obtain high quality ceramics. Although these methods can enhance the quality of KNN ceramic, the cost and complexity also increased. Sintering aids, such as CuO [10, 11] and ZnO [12], can decrease the sintering temperature of ceramics, which prevents the evaporation of alkaline elements. However, the electrical properties were deteriorated seriously. Besides, some ABO_3 perovskite phase, such as $MeTiO_3$ (Me = Ca, Ba, Sr), $LiAeO_3$ (Ae = Nb, Ta) [13–18], were added to KNN to form a solid solution, but the remanent polarization (P_r) values of KNN deteriorated sharply. Recently, Bi-based perovskites with large polarization and multiferroic behavior have been extensively used as additives [19–25]. As one of Bi-based perovskites, $Bi(Mg_{0.5}Ti_{0.5})O_3$ (BMT) exhibits good stable ferroelectricity and is used to modify the electrical properties of $BaTiO_3$ [26–28], $PbTiO_3$ [29–32]. And the ferroelectricity of these materials can be improved.

In this study, BMT was chose to modify the electrical properties of KNN ceramic. The effects of BMT addition on the phase structure, microstructure, and electrical properties of KNN ceramic have been systematically investigated.

2 Experimental

Conventional solid state reaction method was used to prepare the $(1 - x)(K_{0.5}Na_{0.5})NbO_3$–$xBi(Mg_{0.5}Ti_{0.5})O_3$ [abbreviated as $(1 - x)$KNN–xBMT, $0 \leq x \leq 0.04$] ceramics. The raw materials were carbonates and oxide, including Na_2CO_3 (99.8 %), K_2CO_3 (99 %), Nb_2O_5 (99.99 %), Bi_2O_3 (99 %), MgO (98.5 %) and TiO_2 (99.99 %). Stoichiometric proportions of KNN and BMT were mixed in alcohol medium using

zirconia balls for 4 h and calcined at 900 °C for 8 h and 850 °C 4 h, respectively. Subsequently, $(1 - x)$KNN–xBMT powders were weighed and milled in the same way as the raw powders. After drying, the powders were mixed with 5 wt% polyvinyl alcohol (PVA) and pressed into pellets with 12 mm in diameter and 1–2 mm in height by uniaxial pressing under a pressure of 200 MPa. The pellets were then covered with calcined powders of the same composition in order to minimize the volatilization of alkaline elements and sintered at 1,130–1,210 °C for 2.5 h in an alumina crucible. Silver electrodes were fired on the top and bottom surfaces of the samples for the subsequent polarization and measurements. The samples were polarized under a dc field of 3 kV/mm at room temperature in a silicone oil bath for 30 min.

The crystal structures of ceramics were obtained by X-ray diffractometer (XRD) (CuKα1, 1.54059A, Model X'Pert PRO, PANalytical, Almelo, Holland). The microstructure of the sintered samples was observed by a scanning electron microscope (SEM, Philips Electronic Instruments). The densities of samples were measured by Archimedes method. Dielectric property measurement was carried out by impedance analyzer (Agilent 4294A) from room temperature to 550 °C and the frequency range of 40 Hz–1 MHz. The piezoelectric coefficient (d_{33}) was measured using a piezo-d_{33} meter (ZJ-3A, China). The hysteresis loops of selected composition with polarization versus electric field were recorded at room temperature with a ferroelectric test system (TF Analyzer 2000).

3 Results and discussion

The XRD patterns of $(1 - x)$KNN–xBMT ($0 \leq x \leq 0.04$) samples sintered at their optimized temperatures are shown in Fig. 1a. It is clearly seen that all samples exhibit pure perovskite phase and no secondary phase is observed, which indicates that the BMT have completely diffused into the KNN lattice to form a new solid solution. The Orthorhombic (O) and Tetragonal (T) phases can be characterized by splitting of (202)/(020) and (200)/(002) peaks at about 45°, respectively [33, 34]. The diffraction patterns of the samples at about 45° were fitted by Gaussian function, as shown in Fig. 1b. It can be observed that the relative intensities of $(202)_O$ and $(020)_O$ peaks decrease, while the intensities of $(200)_T$ and $(002)_T$ peaks increase with increasing BMT content. Therefore, when $0 \leq x \leq 0.03$, the ceramics have a uniform perovskite phase with orthorhombic structure; as x increases to 0.04, the sample changes to tetragonal structure.

Figure 2 shows the surface microstructures of $(1 - x)$KNN–xBMT ($0 \leq x \leq 0.04$) ceramics. It is distinctly observed that the grain size was affected tremendously by the content of BMT addition. When $x = 0.01$, the grain

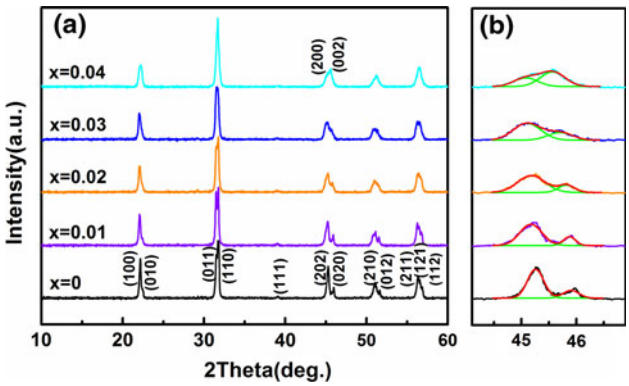

Fig. 1 X-ray diffraction patterns of the $(1 - x)$KNN–xBMT ceramics in the range of 2θ **a** from 10° to 60° and **b** from 44° to 47°

size of samples is larger than pure KNN, which may be attributed to higher sintering temperature from 1,130 to 1,200 °C according to the kinetic grain growth equation expressed as follows [35]

$$\log G = \frac{1}{n}\log t + \frac{1}{n}\left(\log K_o - 0.434\frac{Q}{RT}\right),$$

where G is the average grain size, n is the kinetic grain growth exponent, t is the sintering time, K_o is a constant, Q is the apparent activation energy, R is the gas constant, and T is the absolute temperature. It can be explained that the grain growth was mainly enhanced by increasing sintering temperature. However, when the sintering temperature increased from 1,130 to 1,210 °C, the grain size of samples becomes smaller as x increases from 0.02 to 0.04, which indicates that the addition of BMT is the most important reason to inhibit the grain growth and decrease the grain size. From Table 1, relative density of samples reached the maximum value as x increased to 0.01. However, due to the porous microstructure (as seen in Fig. 2c–e) caused by the more volatilization of K, Na, and Bi at high sintering temperature, the relative density decreased with further increasing x value.

The temperature dependences of the dielectric constant and dielectric loss for $(1 - x)$KNN–xBMT ceramics at 1 MHz are shown in Fig. 3. All ceramics show typical temperature dependence of the dielectric constant. When $0 \leq x \leq 0.03$, two phase transitions corresponding to the orthorhombic-tetragonal (T_{O-T}) and ferroelectric tetragonal-paraelectric cubic (T_{T-C}) can be observed. The peaks at T_{O-T} and T_{T-C} shift to lower temperature with increasing BMT content (as seen in the insert of Fig. 3). The previous researches have shown that a rapid decrease in Curie temperature could be caused by valence mismatch [36, 37]. It is noted that the differences in the valence of KNN and BMT on the A/B cations (K^+, Na^+, Bi^{3+})/(Mg^{2+}, Ti^{4+}, Nb^{5+}) might result in valence mismatch. Therefore, the phase transitions shift to lower temperature with increasing

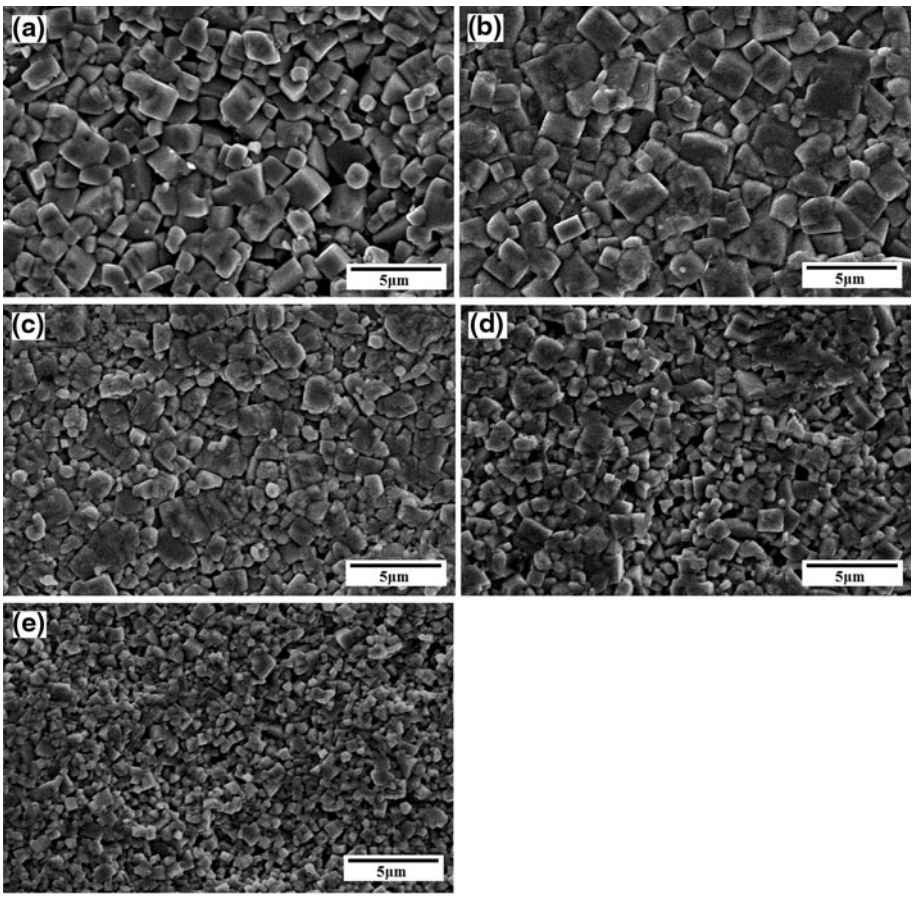

Fig. 2 The SEM images of $(1 - x)$KNN–xBMT ceramics: **a** $x = 0$, 1,130 °C; **b** $x = 0.01$, 1,200 °C; **c** $x = 0.02$, 1,210 °C; **d** $x = 0.03$, 1,210 °C; **e** $x = 0.04$, 1,210 °C

Table 1 The relative densities and electrical properties of $(1 - x)$ KNN–xBMT ceramics

Samples	Relative density (%)	d_{33} (pC/N)	k_p (%)
$x = 0$	97.78	63	21.02
$x = 0.01$	98.89	127	36.58
$x = 0.02$	98.16	82	24.64
$x = 0.03$	96.78	66	17.87
$x = 0.04$	96.32	20	15.66

Theoretical density of $(1 - x)$KNN–xBMT was calculated by mixed rules

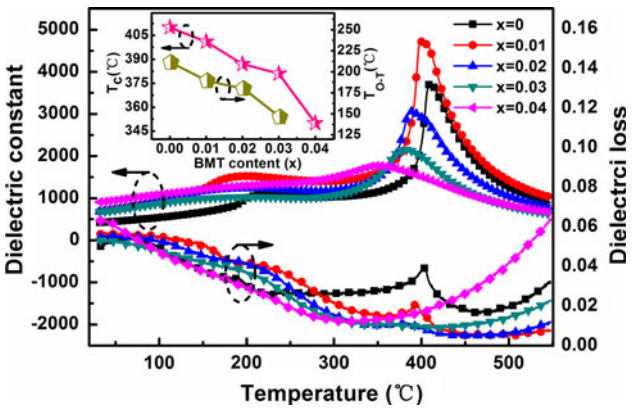

Fig. 3 Temperature dependences of dielectric constant and dielectric loss for $(1 - x)$KNN–xBMT ceramics measured at 1 MHz. *Inset* shows the *curves* of $T_{O\text{-}T}$ and $T_{T\text{-}C}$ versus BMT content

BMT content. When $x = 0.01$, the dielectric constant increased to the maximum value, which may be attributed to the increasing of grain size, leading to the decrease of the grain boundary layer thickness [38]. When x is 0.04, a tetragonal-paraelectric cubic phase transition was observed, which agrees well with analysis of the XRD. These results indicate that the tetragonal phase was stabilized at room temperature [39].

The variations of d_{33} and k_p of the $(1 - x)$KNN–xBMT ceramics as a function of BMT content are shown in Table 1. The d_{33} and k_p were obviously effected by doping BMT. When $x = 0.01$, the maximum values with d_{33} of 127 and k_p of 36.58 % were obtained. The promotion of piezoelectric properties may be related to the increase of relative density which can lower leakage and enhance poling process [40, 41]. In addition, domain rotation is easy for large grains. The large grains may be another reason for improving piezoelectric properties [42–44]. As the x value increases from 0.02 to 0.04, the piezoelectric properties are

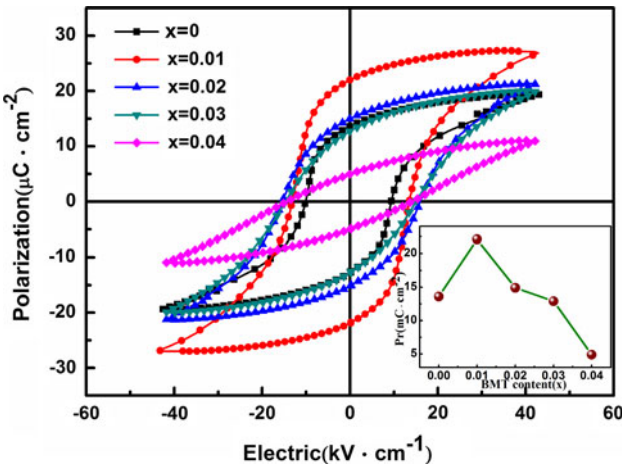

Fig. 4 P–E hysteresis loops of $(1 - x)$KNN–xBMT ceramics. *Inset* shows the *curves* of remnant polarization Pr versus BMT content

deteriorated seriously, which may be attributed to the appearance of reduced relative density and higher leakage.

The hysteresis loops with polarization–electric field (P–E) for the $(1 - x)$KNN–xBMT $(0 \leq x \leq 0.04)$ ceramics are measured at room temperature with 10 Hz, as shown in Fig. 4. Both the remnant polarization (P_r) and coercive field (E_c) exhibited a clear dependency on BMT content. It can be seen that the remnant polarization (P_r) firstly increases and then decreases with increasing x values (as shown in the insert of Fig. 4). The maximum value of the remnant polarization ($P_r = 22.1$ μC/cm^2) and minimum value of coercive field ($E_c = 13.16$ kV/cm) are obtained for $x = 0.01$. The larger P_r and lower E_c might be ascribed to the increase of the relative density which diminishes the leakage current and enhances the polarization [40, 41], and larger grains are easy to domain rotation [42–44]. The decrease of P_r and lower E_c may result from the deviation of Nb^{5+}, Mg^{2+} and Ti^{4+} from the center of the oxygen octahedrons.

4 Conclusions

$(1 - x)$KNN–xBMT $(0 \leq x \leq 0.04)$ lead-free piezoelectric ceramics were synthesized via the solid-state reaction method. The addition of BMT can promote densification and enhance ferroelectric and piezoelectric properties of KNN ceramics. Optimized piezoelectric properties with $d_{33} = 127$ pC/N, $kp = 36.58$ % were obtained for the 0.99KNN–0.01BMT ceramic. Dielectric properties studies showed that both peaks at T_{O-T} and T_C shifted to lower temperature. The researches of polarization versus electric field (P–E) showed good ferroelectric property of $P_r = 22.1$ μC/cm^2 was obtained for $x = 0.01$. The addition of BMT can enhance the density and electrical properties of KNN, which indicates that the $(1 - x)$KNN–xBMT $(0 \leq x \leq 0.04)$ ceramics are promising candidates for the widely used lead-based piezoelectric materials.

Acknowledgments This work was supported by Natural Science Foundation of Guangxi (Nos. 2013GXNSFAA019291 and 2012 GXNSFDA053024), Project of Guangxi Scientific Experiment Center of Mining, Metallurgy and Environment (No. KH2011YB018), Natural Science Foundation of China (Nos. 51102058, 21261007, and 21061004), Research start-up funds Doctor of Guilin University of Technology (No. 002401003282), Project of Department of Science and Technology of Guangxi (Nos. 1348020-11 and 11107006-42) and Guilin (Nos. 20120112-1 and 20120112-2), and Program to Sponsor Teams for Innovation in the Construction of Talent Highlands in Guangxi Institutions of Higher Learning.

References

1. Y. Saito, H. Takao, T. Tani, T. Nonoyama, K. Takatori, T. Homma, T. Nagaya, M. Nakamura, Nature **432**, 84 (2004)
2. B. Malic, J. Bernard, J. Holc, D. Jenko, M. Kosec, J Eur Ceram Soc **25**, 2707 (2005)
3. J.G. Wu, Y.Y. Wang, D.Q. Xiao, J.G. Zhu, Z.H. Pu, Appl Phys Lett **91**, 132914 (2007)
4. Y.L. Wang, X.L. Chen, H.F. Zhou, L. Fang, L.J. Liu, H. Zhang, J Mater Sci Mater Electron **24**, 770 (2013)
5. R.E. Jaeger, L. Egerton, J Am Ceram Soc **45**, 209 (1962)
6. J.F. Li, K. Wang, B.P. Zhang, L.M. Zhang, J Am Ceram Soc **89**, 706 (2006)
7. R.P. Wang, R.J. Xie, T. Sekiya, Y. Shimojo, Mater Res Bull **39**, 1709 (2004)
8. B.P. Zhang, L.M. Zhang, J.F. Li, H.L. Zhang, S.Z. Jin, Mater Sci Forum **475–479**, 1165 (2005)
9. B.P. Zhang, J.F. Li, K. Wang, J Am Ceram Soc **89**, 1605 (2006)
10. D.M. Lin, K.W. Kwok, H.L.W. Chan, Appl Phys Lett **90**, 232903 (2007)
11. H.Y. Park, J.Y. Choi, M.K. Choi, K.H. Cho, S. Nahmw, J Am Ceram Soc **91**, 2374 (2008)
12. S.H. Park, C.W. Ahn, S. Nahm, J.S. Song, Jpn J Appl Phys **43**, L1072 (2004)
13. R.C. Chang, S.Y. Chu, Y.F. Lin, C.S. Hong, P.C. Kao, C.H. Lu, Sens Actuators A **138**, 355 (2007)
14. Y. Guo, K. Kakimoto, H. Ohsato, Jpn J Appl Phys **43**, 6662 (2004)
15. Y.F. Chang, Z.P. Yang, L.L. Wei, B. Liu, Mater Sci Eng A **437**, 301 (2006)
16. R.C. Chang, S.Y. Chu, Y.P. Wong, Y.F. Lin, C.S. Hong, Sens Actuators A **136**, 267 (2007)
17. P. Kumar, P. Palei, Ceram Int **36**, 1725 (2010)
18. Y. Guo, K. Kakimoto, H. Ohsato, Mater Lett **59**, 241 (2005)
19. M.R. Suchomel, P.K. Davies, Appl Phys Lett **86**, 262905 (2005)
20. Y. Uratani, T. Shishidou, F. Ishii, T. Oguchi, Jpn J Appl Phys **44**, 7130 (2005)
21. M.D. Snel, W.A. Groen, G.D. With, J Eur Ceram Soc **25**, 3229 (2005)
22. A. Moure, M. Algueró, L. Pardo, E. Ringgaard, A.F. Pedersen, J Eur Ceram Soc **27**, 237 (2007)
23. J. Wang, J.B. Neaton, H. Zheng, V. Nagarajan, S.B. Ogale, B. Liu, D. Viehland, V. Vaithyanathan, D.G. Schlom, U.V. Waghmare, N.A. Spaldin, K.M. Rabe, M. Wuttig, R. Ramesh, Science **299**, 1719 (2003)
24. A.A. Belik, S. Iikubo, K. Kodama, N. Igawa, S. Shamoto, S. Niitaka, M. Azuma, Y. Shimakawa, M. Takano, F. Izumi, E.T. Muromachi, Chem Mater **18**, 798 (2006)

25. T. Oikawa, S. Yasui, T. Watanabe, H. Yabuta, Y. Ehara, T. Fukui, H. Funakubo, Jpn J Appl Phys **51**, 09LA04 (2012)
26. B. Xiong, H. Hao, S.J. Zhang, H.X. Liu, M.H. Cao, J Am Ceram Soc **94**(10), 3412 (2011)
27. R.T. Sun, X.L. Wang, J. Shi, L. Wang, J Appl Phys A **104**, 129 (2011)
28. B. Lu, X.L. Wang, J. Shi, J Appl Phys **109**, 014117 (2011)
29. S. Sharma, R. Rai, D.A. Hall, J. Shackleton, Adv Mater Lett **3**(2), 92 (2012)
30. T.Y. Ansell, J. Nikkel, D.P. Cann, A. Sehirlioglu, Jpn J Appl Phys **51**, 101802 (2012)
31. R. Rai, A. Sinha, S. Sharmac, N.K.P. Sinha, J Alloys Compd **486**, 273 (2009)
32. R.M. Suchomel, P.K. Davies, J Appl Phys **96**, 4405 (2004)
33. P.Z. Zhang, M.R. Shen, L. Fang, F.G. Zheng, X.L. Wu, J.C. Shen, H.T. Chen, Appl Phys Lett **92**, 222908 (2008)
34. B.L. Cheng, C. Wang, S.Y. Wang, H. Lu, Y.L. Zhou, Z.H. Chen, G.Z. Yang, J Eur Ceram Soc **25**, 2295 (2005)
35. T.Y. Chen, S.Y. Chu, Y.D. Juang, Sens Actuators A **102**, 6 (2002)
36. V.A. Isupov, Phys Status Solidif A **181**, 211 (2000)
37. R.J. Bratton, T.Y. Tien, J Am Ceram Soc **50**, 90 (1967)
38. K.V.R. Prasad, A.R. Raju, K.B.R. Varma, J Mater Sci **29**, 2691 (1994)
39. M. Matsubara, T. Yamaguchi, K. Kikuta, S.C. Hirano, Jpn J Appl Phys **44**(8), 6136 (2005)
40. H.L. Du, Z.M. Li, F.S. Tang, S.B. Qu, Z.B. Pei, W.C. Zhou, Mater Sci Eng B **131**, 83 (2006)
41. X. Zhao, H. Wang, C. Yuan, J. Xu, Y. Cui, J. Ma, J Mater Sci Mater Electron **24**, 1480 (2013)
42. Y.F. Chang, Z.P. Yang, D.F. Ma, Z.H. Liu, Z.L. Wang, J Appl Phys **104**, 024109 (2007)
43. M.S. Kim, S.J. Jeong, J.S. Song, J Am Ceram Soc **90**, 3338 (2007)
44. Y.L. Wang, Y.Q. Lu, M.J. Wu, D. Wang, Y.X. Li, Ceram Int **38**, 295 (2012)